

10-2014

Detection of Bacterial Antigens and Alzheimer's Disease-like Pathology in the Central Nervous System of BALB/c Mice Following Intranasal Infection with a Laboratory Isolate of *Chlamydia pneumoniae*

C. Scott Little PhD

Philadelphia College of Osteopathic Medicine, chrisl@pcom.edu

Timothy A. Joyce

Philadelphia College of Osteopathic Medicine

Christine Hammond

Philadelphia College of Osteopathic Medicine, christineha@pcom.edu

Hazem Matta

Philadelphia College of Osteopathic Medicine, hazemma@pcom.edu

David Cahn

Philadelphia College of Osteopathic Medicine, davidcah@pcom.edu

Recommended Citation

Little, C. Scott PhD; Joyce, Timothy A.; Hammond, Christine; Matta, Hazem; Cahn, David; Appelt, Denah; and Balin, Brian J. PhD, "Detection of Bacterial Antigens and Alzheimer's Disease-like Pathology in the Central Nervous System of BALB/c Mice Following Intranasal Infection with a Laboratory Isolate of *Chlamydia pneumoniae*" (2014). *PCOM Scholarly Papers*. Paper 275.
http://digitalcommons.pcom.edu/scholarly_papers/275

See next page for additional authors

Follow this and additional works at: http://digitalcommons.pcom.edu/scholarly_papers

 Part of the [Nervous System Diseases Commons](#), and the [Neurology Commons](#)

Authors

C. Scott Little PhD, Timothy A. Joyce, Christine Hammond, Hazem Matta, David Cahn, Denah Appelt, and Brian J. Balin PhD

Detection of bacterial antigens and Alzheimer's disease-like pathology in the central nervous system of BALB/c mice following intranasal infection with a laboratory isolate of *Chlamydia pneumoniae*

Christopher Scott Little, Timothy A. Joyce, Christine J Hammond, Hazem Matta, Denah M. Appelt, Brian Joseph Balin and David Cahn

Journal Name: Frontiers in Aging Neuroscience
ISSN: 1663-4365
Article type: Original Research Article
Received on: 05 Aug 2014
Accepted on: 18 Oct 2014
Provisional PDF published on: 18 Oct 2014
www.frontiersin.org: www.frontiersin.org
Citation: Little CS, Joyce TA, Hammond CJ, Matta H, Appelt DM, Balin BJ and Cahn D(2014) Detection of bacterial antigens and Alzheimer's disease-like pathology in the central nervous system of BALB/c mice following intranasal infection with a laboratory isolate of *Chlamydia pneumoniae*. *Front. Aging Neurosci.* 6:304. doi:10.3389/fnagi.2014.00304
Copyright statement: © 2014 Little, Joyce, Hammond, Matta, Appelt, Balin and Cahn. This is an open-access article distributed under the terms of the [Creative Commons Attribution License \(CC BY\)](http://creativecommons.org/licenses/by/2.0/). The use, distribution and reproduction in other forums is permitted, provided the original author(s) or licensor are credited and that the original publication in this journal is cited, in accordance with accepted academic practice. No use, distribution or reproduction is permitted which does not comply with these terms.

This Provisional PDF corresponds to the article as it appeared upon acceptance, after rigorous peer-review. Fully formatted PDF and full text (HTML) versions will be made available soon.

1 **Detection of bacterial antigens and Alzheimer’s disease-like**
2 **pathology in the central nervous system of BALB/c mice**
3 **following intranasal infection with a laboratory isolate of**
4 *Chlamydia pneumoniae*

5
6 **Running Title:** AD-like Pathology following Cpn Infection

7
8 **Authors and Affiliations:**

9
10 C. Scott Little, Ph.D.¹⁺, Timothy A. Joyce, M.S., M.D.¹⁺, Christine J. Hammond, M.S.²⁺,
11 Hazem Matta, D.O.⁺, David Cahn, D.O.⁺, Denah M. Appelt, Ph.D.¹⁺, Brian J. Balin,
12 Ph.D.¹⁺

13
14 ¹Department of Bio-Medical Sciences, ²Division of Research, ⁺ Center for Chronic
15 Disorders of Aging, Philadelphia College of Osteopathic Medicine, Philadelphia, PA,
16 USA.

17
18 **Correspondence:**

19 *C. Scott Little, Ph.D
20 Philadelphia College of Osteopathic Medicine
21 Department of Bio-Medical Sciences
22 4170 City Ave
23 Philadelphia, PA, 19131, USA
24 ChrisL@pcom.edu

25
26 Abstract Characters count: 1,960

27 Manuscript word count: 6,965

28 Number of figures: 4

29 Number of Tables: 1

30 **ABSTRACT**

31 Pathology consistent with that observed in Alzheimer's disease (AD) has previously been
32 documented following intranasal infection of normal wild-type mice with *Chlamydia*
33 *pneumoniae* (Cpn) isolated from an AD brain (96-41). In the current study, BALB/c mice
34 were intranasally infected with a laboratory strain of Cpn, AR-39, and brain and olfactory
35 bulbs were obtained at 1-4 months post-infection (pi). Immunohistochemistry for amyloid
36 beta or Cpn antigens was performed on sections from brains of infected or mock-infected
37 mice. *Chlamydia*-specific immunolabeling was identified in olfactory bulb tissues and in
38 cerebrum of AR-39 infected mice. The Cpn specific labeling was most prominent at 1
39 month pi and the greatest burden of amyloid deposition was noted at 2 months pi, whereas
40 both decreased at 3 and 4 months. Viable Cpn was recovered from olfactory bulbs of 3 of 3
41 experimentally infected mice at 1 and 3 months pi, and in 2 of 3 mice at 4 months pi. In
42 contrast, in cortical tissues of infected mice at 1 and 4 months pi no viable organism was
43 obtained. At 3 months pi, only 1 of 3 mice had a measurable burden of viable Cpn from the
44 cortical tissues. Mock-infected mice (0 of 3) had no detectable Cpn in either olfactory
45 bulbs or cortical tissues. These data indicate that the AR-39 isolate of Cpn establishes a
46 limited infection predominantly in the olfactory bulbs of BALB/c mice. Although infection
47 with the laboratory strain of Cpn promotes deposition of amyloid beta, this appears to
48 resolve following reduction of the Cpn antigen burden over time. Our data suggest that
49 infection with the AR-39 laboratory isolate of Cpn results in a different course of amyloid
50 beta deposition and ultimate resolution than that observed following infection with the
51 human AD-brain Cpn isolate, 96-41. These data further support that there may be
52 differences, possibly in virulence factors, between Cpn isolates in the generation of
53 sustainable AD pathology.

54

55 **INTRODUCTION**

56 Alzheimer's disease (AD) is the most common dementia in the US, accounting for 50 to 70
57 percent of cases. More than 5 million Americans are living with a diagnosis of AD as of
58 2013 with 90-95% of cases in the 65 and older segment of the population. Early stage of
59 disease involves memory impairment (Fargo and Bleiler. 2014). In the advanced stages of
60 AD, individuals require assistance with daily activities and, ultimately, in the final stage
61 become bed-bound and are reliant on around-the-clock care (Hebert, *et al.* 2003). AD is a
62 fatal disorder with the progression from the earliest symptoms to total functional
63 dependency and death in an untreated person often occurring within 8-10 years post
64 diagnosis (Fargo and Bleiler. 2014) .

65 Although much is known about the disease process and progression of AD, the initiating
66 factors or cause(s) of the disease still remain a mystery. AD has an early onset familial
67 form that is primarily driven by autosomal dominant genetic alterations in genes encoding
68 the beta amyloid precursor protein, as well as the loci encoding presenilins 1 and 2 (Goate,
69 *et al.* 1991; Levy-Lahad, *et al.* 1995; Rogaev, *et al.* 1995; Wolfe. 2007). Transgenic mouse
70 models have been developed to induce enhanced β -amyloid production and subsequent
71 deposition of β -amyloid (Hall and Roberson. 2012; Wisniewski and Sigurdsson. 2010),
72 and serve as models for early onset AD, which accounts for ~3-5 % of all reported cases.
73 One important issue that cannot be addressed using these model systems is how to target
74 the early initiating events in sporadic late-onset AD and not just the "tombstone" lesions
75 that are the result of a long chain of pathological processes (Wisniewski and Sigurdsson.

76 2010). In this regard, animal models that mimic the sporadic late-onset form of AD have
77 been developed, but these are hampered by the lack of understanding of the primary factors
78 that promote the deposition of β -amyloid. Currently, models that experimentally induce
79 AD-like pathology use bacterial toxins such as streptozotocin (Labak, *et al.* 2010), chronic
80 stress (Alkadhi, *et al.* 2010), or colchicine to chemically induce damage (Kumar, *et al.*
81 2007) to the CNS to initiate pathology. As several infectious agents, including *Chlamydia*
82 *pneumoniae* (Cpn), have been proposed to enhance risk or play a causal role in AD
83 (Gerard, *et al.* 2006; Balin, *et al.* 1998), animal models have been developed to study the
84 effects of this infection (Little, *et al.* 2004; Little, *et al.* 2005) with regards to AD-like
85 pathology. However, there remains a dearth of experimental animal systems that
86 accurately model sporadic late-onset AD, leaving the scientific community with few
87 options to address key questions related to the initiation/ progression of late-onset disease.
88

89 The identification of Cpn in AD brain tissue (Balin, *et al.* 1998) was a stimulus to
90 investigate the potential role that this organism plays in the induction and progression of
91 late-onset AD and led to the establishment of a mouse model to investigate this occurrence
92 (Little, *et al.* 2004). In the original experimental system, BALB/c mice were infected with
93 Cpn isolated from human AD brain autopsy tissue. The isolate of Cpn, 96-41, was
94 propagated in HEP-2 cells and then introduced into 3 month old BALB/c mice via
95 intranasal inoculation; brain tissue was analyzed at monthly time points up through 3
96 months pi following intranasal delivery.
97

98 Our first study utilized the human AD-brain isolate of Cpn to induce AD-like pathology in
99 non-transgenic mice (Little, *et al.* 2004), and was designed to address Koch's postulates.
100 The first postulate requires that the infectious organism be isolated from tissues of an
101 affected individual. In this particular case, the first postulate is satisfied, but for other cases
102 of the disease this issue is still debate (Itzhaki, *et al.* 2004). To satisfy Koch's second
103 postulate, the pathogen must be isolated from a diseased organism and grown in pure
104 culture. Cpn was isolated post-mortem from human AD-brain tissue and grown in culture
105 (although culture required a eukaryotic cell as this is an obligate intracellular bacterium).
106 Third, the organism was introduced into a mouse, and induced pathology consistent with
107 AD, while uninfected mice did not display the same pathology. Fourth, the organism was
108 identified in the tissues of affected mice, but was not re-isolated from the tissue. Thus,
109 Koch's postulates were used as a general guide, and although difficult to use in their purest
110 sense when addressing any intracellular infection, our findings support the hypothesis that
111 Cpn infection can induce β -amyloid deposition in the brain and contribute directly to
112 pathogenesis.
113

114 In mice infected with Cpn in our first report, β -amyloid deposits were identified as early as
115 two months pi, with the greatest number of deposits identified at three months pi. The
116 number and size of amyloid deposits increased over time, thus the development of AD-like
117 pathology appeared to be progressive. The experimental induction of mouse derived
118 β -amyloid deposits in inbred BALB/c mice (not genetically modified) at 5 and 6 months of
119 age (2 and 3 months pi) indicates that infection can trigger the production and deposition of
120 β -amyloid in the mouse brain. In contrast, in transgenic mouse models used to study AD, 6
121 months of age is very early to observe substantial amyloid deposits, yet we observed

122 substantial pathology 2 months after introduction of the infectious agent into
123 non-transgenic animals. Cpn is a respiratory pathogen and was introduced into mice via an
124 intranasal inoculation. This is the natural route of infection and the organism can be
125 responsible for an acute respiratory illness. The respiratory infection appears to precede
126 dissemination to other organ systems (Little, *et al.* 2005) and age is an important factor in
127 the host's ability to control the dissemination, with even greater spread with the advent of
128 immunosenescence in older animals.

129
130 In contrast with the initial report associating Cpn with the induction of AD-like pathology
131 in the brains of BALB/c mice (Little, *et al.* 2004), the current study was performed with a
132 respiratory isolate and common laboratory strain of Cpn, AR-39. The purpose was to
133 determine if this well-studied laboratory isolate of Cpn would induce pathology in a similar
134 manner and to the same degree over a similar time course, as that observed for the human
135 CNS isolate used previously. This approach will inform potential differences in outcomes
136 when infecting mice with Cpn originally isolated from lung tissues and used as a laboratory
137 isolate as compared to that from human AD brain.

138 139 **MATERIALS AND METHODS**

140 **HEp-2 cell line:** The human epithelial, HEp-2, cell line (ATCC, Rockville MD) was
141 maintained in MEM supplemented with 10% fetal bovine serum (FBS) (Cell Gro
142 Mediatech, Inc, Manassas, VA), 5mM L-Glutamine (Thermo Fisher Scientific, Pittsburgh,
143 PA) at 37°C and 5% CO₂. 1-2 x 10⁵ cells were plated in a T25 tissue culture flask
144 (Thermo Fisher Scientific, Pittsburgh, PA) and passaged as needed prior to collection for
145 the propagation of Cpn.

146
147 **Propagation and purification of *Chlamydia pneumoniae*:** *Chlamydia pneumoniae*
148 (Cpn), AR-39 isolate, was obtained from the ATCC (ATCC, Rockville, MD) and
149 propagated in the HEp-2 cell line similar to the technique described for the Cpn brain
150 isolate, 96-41 (Little, *et al.* 2004; Campbell, *et al.* 1991). Prior to infection of BALB/c mice,
151 homogenates of 72 h culture supernatants and Cpn infected HEp-2 cells were sonicated for
152 30 seconds and passed through a series of filter membranes with decreasing pore size to
153 collect the elementary bodies. The organism was resuspended in Hanks Balanced Salt
154 Solution (HBSS), aliquoted, and stored at -80 C. The quantitation of inclusion forming
155 units subsequently was determined following infection of HEp-2 epithelial cells with a
156 series of 10 fold serial dilutions of the concentrated organism. The inclusions were
157 identified by immunofluorescence using a Chlamydia-specific antibody directly
158 conjugated to FITC (ImagenTM; DAKO, Carpinteria, CA). Aliquots were diluted in HBSS
159 to a working concentration for the intranasal infection of mice.

160
161 **Mice:** Six week old female BALB/cJ mice were purchased from Jackson Laboratories (Bar
162 Harbor, ME) and acclimated for 2 weeks prior to use. Mice were housed in groups of 2-3 in
163 HEPA-filter caged racks, with infected mice housed separately from uninfected mice,
164 within the containment facility at Philadelphia College of Osteopathic Medicine. All
165 animal husbandry was performed using Biosafety Level 2 precautions and in a Class II
166 biosafety cabinet. Mice were fed food and water ad libitum. All animal protocols were
167 approved by the IACUC at PCOM.

168

169 **Infection of mice with *Chlamydia pneumoniae*:** Under manual restraint, 8 week old,
170 female BALB/cJ mice were inoculated intranasally with 5×10^5 inclusion forming units of
171 the AR-39 isolate of Cpn diluted in 50 μ l of HBSS. Six mice were inoculated at 8 weeks of
172 age for each time point and the brains were analyzed at 1, 2, 3 and 4 months post infection.
173 Four age and sex matched mice were mock-infected with vehicle alone, HBSS, as a control
174 for each time point. At each time point, 3 experimentally-infected and 2 mock-infected
175 control mice were anesthetized, cardiac-perfused and organs were collected and immersion
176 fixed in 4 % paraformaldehyde for embedding, sectioning and immunohistochemical
177 analysis. The remaining 3 experimentally-infected and 2 mock-infected control mice at
178 each time point other than for 2 month animals for which frozen tissue was not available
179 were euthanized and organs were collected and snap-frozen in liquid nitrogen and then
180 stored at -80 C until analysis for detection and quantification of viable organism.

181

182 **Recovery and quantification of *Chlamydia pneumoniae*:** Quantification of viable Cpn
183 was performed in an identical manner to our previous report (Little et al 2005) (Little, *et al.*
184 2005) in the following manner. Frozen tissue was thawed and a 10% weight to volume
185 homogenate was prepared in serum-free minimal essential medium (MEM) (Thermo
186 Fisher Scientific, Pittsburgh, PA) supplemented with 2mM Glutamine. Serial ten-fold
187 dilutions (in 200 μ L) were added to 4 well Lab Tech chamber slides (Naperville, IL) on
188 which HEp-2 cells were previously plated. Negative control wells contained cells
189 mock-infected with medium alone. The chamber slides were incubated at 37°C in 5% CO₂
190 for 2.5 hrs, washed with HBSS and refilled with fresh complete medium supplemented
191 with 2 μ g/ml cycloheximide (Sigma-Aldrich, St. Louis, MO) followed by incubation for 48
192 hrs at 37°C. After incubation, slides were washed with HBSS, fixed in 50% methanol at RT
193 for 20 min, washed twice in HBSS, and labeled with a 1:10 dilution of FITC-conjugated
194 Chlamydia-specific antibody (ImagenTM; DAKO, Carpinteria, CA) for 90 min in the dark
195 at 37°C. Slides were washed in phosphate buffered saline (PBS) and counterstained with a
196 2 μ g/ml of bisBenzamide (Sigma-Aldrich, St. Louis, MO) in PBS for 1 min, washed in
197 PBS and coverslipped with aqueous mounting medium (ImagenTM; DAKO, Carpinteria,
198 CA). All titers are calculated as inclusion forming units (IFU)/ml of 10% weight to volume
199 tissue homogenate.

200

201 **Antibodies:** The following *Chlamydia*-specific antibodies were generated in mice:
202 RDI-PROAC1p (Research Diagnostics Incorporated, Flanders, NJ) (AC1P) (monoclonal
203 I_gG) specific for *Chlamydia* lipopolysaccharide used at a dilution of 1:10 (5 μ g/ml), M6600
204 (DakoCytomation, Carpinteria, CA) (monoclonal I_gG) specific for Cpn major outer
205 membrane protein used at a dilution of 1:10 (10 μ g/ml), and 10C-27 (Fitzgerald, Concord,
206 MA) (monoclonal I_gG) specific for Cpn used at a dilution of 1:100 (1 μ g/ml). Additionally,
207 B65256R (Biodesign International, Saco, ME) (B56R) specific for *Chlamydia* purified
208 elementary bodies was generated in rabbit and used at a dilution of 1:200 (2 μ g/ml). Both
209 secondary antibodies specific for either mouse, AP-Goat anti-mouse IgG conjugate
210 (Zymed Laboratories, San Francisco, CA), or rabbit, AP-Goat anti-rabbit IgG conjugate
211 (Zymed Laboratories, San Francisco, CA), were used at a concentration of 2 μ g/ml. All
212 antibodies were diluted to working concentration in 2% FBS/PBS blocking buffer (Thermo
213 Fisher Scientific, Pittsburgh, PA). For the detection of A β amyloid, the following

214 antibodies were used at a recommended concentration of 2 µg/ml: a rabbit polyclonal
215 antibody specific for the carboxyl-terminal fragment of Aβ amyloid 1-42 (catalogue:
216 A1976 Oncogene Research Products, Boston, MA), and a mouse monoclonal antibody
217 (4G8) to the 17-24 amino acid peptide of human Aβ amyloid 1-42 (catalogue:9220-05
218 Signet Laboratories Inc., Dedham, MA). For all amyloid specific immunolabeling,
219 secondary antibodies consisted of HRP conjugated sheep anti-Mouse IgG (H + L) or
220 donkey anti-rabbit IgG (H + L). Antibodies were used at a dilution of 1:300 as
221 recommended by the supplier (Amersham Biosciences, Piscataway, NJ and Life
222 Technologies, Inc, Grand Island, NY).

223

224 **Immunohistochemistry:** Brain sections from experimental and control mice were
225 immunolabeled for Aβ amyloid or Cpn antigen at 1, 2, 3, and 4 months post infection using
226 the aforementioned antibodies. Coronal sections were deparaffinized with xylene (Thermo
227 Fisher Scientific, Pittsburgh PA) rehydrated in a series of graded alcohol solutions
228 (Electron Microscopy Sciences, Fort Washington, PA), followed by de-ionized (DI) H₂O.
229 Slides were then placed in Citra antigen retrieval buffer (BioGenex, San Ramon, CA) and
230 steamed in a 2100 Retriever (Pick Cell Laboratories, Amsterdam, Netherlands) for 20 min
231 at high pressure and temperature (120° C). Slides were then rinsed with PBS pH 7.4
232 (Sigma-Aldrich, St Louis, MO) 3 x 5 minutes. Endogenous peroxidase activity was
233 quenched utilizing a 3% solution of H₂O₂/PBS (Thermo Fisher Scientific, Pittsburgh, PA)
234 for 5 min at RT. Sections were rinsed 1 x 5 min in PBS and blocked 3 x in 2% heat
235 inactivated fetal bovine serum (FBS)/PBS. A total of 30 coronal brain sections, 10 sets of 3
236 sections (1 per antibody), were immunolabeled per mouse. The sections were spaced
237 equally (approximately every 70-100 microns in brain tissue) from rostral (bregma +
238 2.22mm) to caudal (bregma -5.88mm) in order to provide samples representative of the
239 regions spanning the entire brain of each mouse. Slides receiving Chlamydia-specific
240 primary antibodies B56R or a cocktail of 10C-27, AC1P, M6600 were applied to tissue
241 sections and placed in a humidified chamber at 37 °C for 90 min. The sections were rinsed
242 3 x 5 min each and then blocked 3 x 15 min each in 2% FBS/PBS, and incubated with
243 appropriate secondary antibodies in a humidified chamber for 1 hour at 37 °C. Following
244 incubation, sections were rinsed with DI H₂O 3 x 5 min and developed using alkaline
245 phosphatase new magenta for 15 min (BioFX, Owings Mills, MD) at RT. Sections were
246 rinsed in DI H₂O 3 x 5 min followed by one PBS rinse for 5 min. Acidified Harris's
247 Hematoxylin (Thermo Fisher Scientific, Pittsburgh, PA) was applied to sections for 1 min.
248 One DI H₂O rinse followed counterstaining and the sections were contrasted in PBS for 5
249 min. Finally, the sections were rinsed with DI H₂O 3 x 5 min, air dried, and crystal
250 mounted (BioMeda, Foster City, CA). Once dry, the sections were permounted and
251 coverslipped.

252

253 Slides receiving mouse primary antibodies were blocked in mouse on mouse (M.O.M.)
254 IgG blocking reagent (Vector M.O.M. kit, Vector Laboratories, Burlingame, CA) for 1 hr
255 at RT, rinsed, and incubated for 5 min in the M.O.M. blocking buffer. For all sections, the
256 primary antibodies were incubated overnight at 4⁰C. The sections were rinsed in PBS 3 x
257 for 5 min each, blocked 3 x for 15 min each in 2% FBS/PBS, and incubated with
258 appropriate secondary antibodies in a humidified chamber for 2 h at RT. The sections
259 labeled with anti-amyloid antibodies were rinsed with PBS 3 x for 10 min each and

260 visualized with 3, 3'-Diaminobenzidine (DAB) (Sigma FAST™, Sigma-Aldrich, St. Louis,
261 MO). Sections were rinsed with dH₂O, counterstained with Harris' Alum Hematoxylin
262 (EM Sciences Harleco^R, EM Industries, Inc., Hawthorne, NY), and permounted.

263

264 **Microscopic Analysis:** Digital images were captured using Image-Pro Plus Phase 3
265 Imaging System software (Media Cybernetics, Silver Spring, MD) on a Nikon Eclipse
266 E800 microscope using a Spot RT Camera (Diagnostic Instruments, Sterling Heights, MI).

267

268 **Statistical Analysis:**

269 Statistical analysis was performed using the student t-test followed by pair-wise testing of
270 uninfected (n=8) relative to each experimental infected timepoint (n=3) using Microsoft
271 excel statistical analysis software and *P* values of < 0.05 which were considered
272 significant.

273

274 **RESULTS**

275 **Recovery of infectious *Chlamydia pneumoniae* from olfactory bulbs and cerebrum:**

276 Olfactory bulbs and cerebral tissues were dissected from BALB/c mice following
277 euthanization, snap frozen, and homogenized prior to incubation with HEp-2 cells in
278 culture to determine if detectable levels of viable Cpn could be recovered from the central
279 nervous system. Ten-fold serial dilutions of the homogenized tissues were incubated with
280 HEp-2 cells to determine the amount of viable infectious Cpn present in the tissues at 1, 3
281 and 4 months pi. Tissue from the 2 month animal was not available. Infectious Cpn was
282 recovered and quantified from 3 of 3 olfactory bulbs at 1 month pi, ranging from 3×10^3 to
283 3×10^5 IFU/ml of tissue homogenate (Fig 1a). At 3 months pi, Cpn was detected in 3 of 3
284 olfactory bulbs with a range of 2×10^5 to 3×10^6 IFU/ml of tissue homogenate (Fig 1a). At
285 4 months, Cpn was detected in 2 of 3 olfactory bulbs with a range of 0 to $\sim 2 \times 10^6$ IFU/ml
286 tissue homogenate (Fig. 1a). Of the 3 olfactory bulbs tested from the mock infected
287 animals, no Cpn was recovered. In contrast to the olfactory bulbs, Cpn was not recovered
288 from the brain tissue (cerebrum) at 1 and 4 months pi, although at 3 months, Cpn was
289 recovered and quantified at 3×10^4 IFU/ml of tissue from 1 of 3 brains (Fig. 1b). This same
290 mouse had 3×10^5 IFU/ml in the olfactory bulb as noted above. With regards to brain
291 tissues analyzed from the 3 control animals, no Cpn was detected.

292

293 **Identification and distribution of *Chlamydia pneumoniae* antigen in the central**
294 **nervous system:** Cpn antigen was detected in olfactory bulb tissues at 1 and 3 months pi
295 using antibodies specific for Cpn LPS and outer membrane proteins. Representative
296 immunolabeling for Cpn in these tissues at 1 month pi was principally intracellular (Fig.2).
297 The labeling profiles consisted of large intracellular vacuoles, often perinuclear with
298 prominent well-defined inclusions. Furthermore, Cpn antigen labeling (LPS and outer
299 membrane proteins) was documented within the cerebrum with a quantitative analysis of
300 10 total slides per animal distributed rostral to caudal with distances measured from
301 Bregma (Table 1). Intracellular immunolabeling was observed to be both perinuclear and
302 diffuse in the cytoplasm with very few clearly documentable intracellular inclusions (Fig.
303 3). However, upon close examination, punctate immunolabeling was observed in
304 numerous cells (Fig. 3c,e).

305

306 **Table 1:** Location of *Chlamydia pneumoniae* immunoreactivity and A β 1-42 amyloid
 307 deposits over 4 months post infection within brains of Cpn-infected mice. (A) The
 308 location and number of immunoreactive amyloid deposits or Cpn antigen is designated in
 309 millimeters (section location in mm) rostral or caudal to the mouse bregma. (B) Statistical
 310 analysis of Cpn-specific immunoreactivity and A β 1-42 immunoreactive deposits from
 311 infected and uninfected mouse brains. For each time point, N = animals analyzed, *
 312 indicate statistical significance.

313
 314 **Table 1**
 315 **A**

	Bregma									Total	
	2.22	1.7	0.38	-1.28	-2.75	-3.8	-4.92	-5.46	-5.88	Inf	Un
1 Mo Cpn	22	10	22	18	23	42	9	6	2	154	24
Amyloid	0	1	0	3	3	0	2	1	0	10	0
2 Mo Cpn	18	15	19	5	26	21	20	10	0	134	14
Amyloid	8	30	11	16	31	43	35	6	0	180	12
3 Mo Cpn	11	11	13	22	5	9	9	4	7	91	10
Amyloid	0	9	14	7	4	3	3	11	2	53	10
4 Mo Cpn	0	11	13	15	13	10	10	1	3	76	9
Amyloid	0	0	3	6	3	1	5	1	0	19	5
Cpn	51	47	67	60	67	82	48	21	12	455	57
Amyloid	8	33	12	5	32	19	33	1	0	143	27

316
 317 **B**
 318

time p.i.	Chlamydia-specific immunoreactivity				Amyloid deposits				
	uninfected n=2		infected n=3		time p.i.	uninfected n=2		infected n=3	
	mean	s.d.	mean	s.d.		mean	s.d.	mean	s.d.
1	12	5.65	51.33*	32.01	1	0	0	3.33	1.167
2	7	2.83	44.67*	33.56	2	6	1	60*	8
3	5	1.41	30.33*	12.06	3	5	1	17.67*	0.67
4	4.50	0.71	25.33	24.21	4	2.5	1.5	6.33	2.167
ALL	7.13	4.02	37.92	21.22	ALL	3.38	2.28	21.83	19.08

319
 320 Quantitative analysis of Cpn antigen in the brain at 1 through 4 months post-intranasal
 321 inoculation revealed peak Cpn antigen burden (154 immunoreactive profiles) at 1 month
 322 (Table 1A). Cpn-specific immunoreactivity demonstrated a step-wise decrease at 2, 3, and
 323 4 months pi with 134, 91, and 76 immunoreactive profiles, respectively. With regards to
 324 specific coordinates in the brain, the greatest Cpn antigen burden (ie, 42 Cpn
 325 immunoreactive profiles) was documented at 1 month in multiple sections 3.8 mm caudal

326 to bregma. These sections contain the entorhinal cortex, perirhinal cortex, hippocampus,
327 and amygdala, all regions affected in Alzheimer's disease. A low but detectable number of
328 non-specific Cpn immunoreactive sites were detected within mock-infected control mouse
329 brain tissue with an average number of 0.355/section analyzed. The mean number of
330 immunoreactive sites identified was 7.125/ mouse +/- 4.01 and based upon the results of
331 the student t-test a statistically significant difference ($p < 0.05$) was observed between
332 experimentally infected tissue and mock-infected control mouse tissue at all timepoints
333 analyzed; 1 month p.i. (51.33 +/- 32.01), 2 months p.i. (44.67 +/- 33.56), and 3 months
334 p.i.(30.33 +/- 12.06). No statistically significant difference was observed in the 4 month
335 p.i. (25.33 +/- 24.21) experimental group relative to uninfected control tissue (Table 1 B).

336

337 **Identification and distribution of amyloid antigen in the central nervous system**

338 Antibodies specific for amyloid beta 1-40 ($A\beta$ 1-40) and amyloid beta 1-42 ($A\beta$ 1-42) were
339 used to determine if immunoreactive deposits could be detected in mock infected controls
340 and experimentally infected BALB/c mice. A limited number of $A\beta$ 1-40 immunoreactive
341 deposits were observed exclusively in the brains of experimentally infected mice at 2
342 months post-infection (data not shown). No $A\beta$ 1-40 deposits were detected in the brains of
343 any control mice at any timepoint nor in experimentally infected mice at 1, 3 and 4 months
344 post infection.

345

346 Quantitative analysis of amyloid burden revealed the highest number of $A\beta$ 1-42
347 immunoreactive deposits (43) at 2 months pi 3.8 mm caudal to bregma, similar to Cpn
348 immunoreactivity at 1 month pi (Table 1A). Overall $A\beta$ 1-42 immunoreactivity was
349 greatest at 2 month pi, having been minimal at 1 month pi and decreasing at 3 and 4 months
350 pi. As noted above, these sections contain the entorhinal cortex (Ect), perirhinal cortex
351 (Prh), cerebral peduncle (Cp), hippocampus, and amygdala, all regions affected in
352 Alzheimer's disease (see Fig 4 for $A\beta$ 1-42 immunoreactive deposits). A low but
353 detectable number of amyloid-specific immunoreactive sites were detected within
354 mock-infected control mouse brain tissue at 2, 3, and 4 months p.i. with an average number
355 of 0.17/section analyzed. The mean number of immunoreactive sites identified was 3.38/
356 mouse +/- 2.28 and based upon the results of the student t-test a statistically significant
357 difference ($p < 0.05$) was observed between experimentally infected tissue and
358 mock-infected control mouse tissue at 2 months p.i. (60/mouse +/- 8) and 3 months p.i.
359 (17.67 +/-0.67). No statistically significant difference was detected at 1 month p.i. (3.33 +/-
360 1.17) or 4 months p.i. (21.83 +/- 19.08) (Table 1 B).

361

362 **DISCUSSION**

363 This study was designed as a follow-up investigation to the initial report of experimental
364 induction of AD-like pathology in BALB/c mice following intranasal inoculation with *C*
365 *pneumoniae* (Little, *et al.* 2004). The key difference in the current study as compared to
366 that by Little et al 2004 was that the AR39 respiratory lab strain was used to evaluate the
367 effects in the brain as compared to the 96-41 brain strain used in the initial report.
368 *Chlamydia*- specific immunolabeling was identified in olfactory bulb tissues and in brains
369 (cortical tissues) of AR-39-infected mice. The Cpn-specific labeling was most prominent
370 at 1 month post-infection (pi) and the greatest burden of amyloid deposition was noted at 2
371 months pi, whereas both decreased at 3 and 4 months pi. The majority of amyloid deposits

372 at these times were immunoreactive for A β 1-42. Interestingly, a limited number of A β
373 1-40 immunoreactive deposits also was identified (data not shown), but only at the 2 month
374 time point, the time of peak amyloid burden. Viable Cpn was recovered from the olfactory
375 bulb tissues of 3 of 3 experimentally infected mice at 1 and 3 months pi, and 2 of 3 at 4
376 months pi. In contrast, in cerebral cortical tissues of experimentally infected mice, only at 3
377 months pi did 1 of 3 mice have a measurable burden of viable Cpn. Mock-infected control
378 mice had no detectable Cpn in either olfactory bulbs (0 of 3) or cortical tissues (0 of 3).
379 These data indicate that, following intranasal infection, the AR-39 respiratory isolate of
380 Cpn establishes a limited infection predominantly in the olfactory bulbs of BALB/c mice.
381 Furthermore, although infection with the laboratory strain of Cpn promotes deposition of
382 A β amyloid, this appears to resolve following reduction of the Cpn antigen burden over
383 time.

384
385 In our current study, brains were analyzed at 1 through 4 months pi by immunohisto-
386 chemistry with antibodies specific for Chlamydia antigen and antibodies specific for
387 A β -amyloid 1-42. Similar to the initial report utilizing the 96-41 human AD-brain isolate,
388 no substantial amyloid deposits were observed at 1 month pi and a limited degree of
389 AD-like pathology was identified at 2 months pi with AR-39. In contrast to the original
390 study utilizing the brain isolate, at 4 months pi AD-like pathology was comparable to that
391 observed in mock infected mice and infected mice at 1 month pi, suggesting that the degree
392 of pathology had decreased between 2 through 4 months pi. Identification and quantitative
393 analysis of Chlamydia antigen burden indicated that peak Chlamydia antigen burden
394 preceded peak amyloid deposition. The greatest Chlamydia antigen burden in brains of
395 infected BALB/c mice was noted at 1 month pi, and decreased at 2 through 4 months pi,
396 whereas peak amyloid burden was at 2 months pi, and decreased thereafter. Taken
397 together, the burden of Chlamydia antigen and number of amyloid deposits suggests that
398 Cpn infection serves as a primary stimulus for A β -amyloid processing and deposition in
399 brain tissues. While consistent co-localization of amyloid with Chlamydia antigen was not
400 apparent, both were present in the same regions at times consistent with AD-like
401 pathology. As the course of infection preceded the course of pathology development,
402 infection may serve as a stimulus for inflammation as well as for beta amyloid production
403 and deposition. Precedence for infection in exacerbating AD-like pathology has been
404 reported for other types of infections in different animal models (McManus, *et al.* 2014;
405 Wang, *et al.* 2014). Once the infection has been controlled or resolved completely, levels
406 of soluble amyloid apparently decrease presumably following internalization by glial cells
407 (Hawkes, *et al.* 2012) and/or washout into the blood, thereby resulting in fewer deposits
408 documented at the 3 and 4 month timepoints. These findings support our contention that
409 laboratory strains of Cpn from respiratory infections as compared to Cpn brain isolates are
410 less capable of creating long-standing damage in the CNS. In this regard, at the present
411 time, we do not know what inoculum of Cpn is sufficient to not only initiate but to promote
412 chronic human disease, nor do we understand potentially different virulence factors of Cpn
413 isolated from different tissue sites. Our animal studies do support our contention that
414 infection (even in modest titers - 10^5 organisms), specifically through an intranasal route,
415 can initiate changes in the brain consistent with early AD-like pathology.

416
417 In mice infected with the 96-41 Cpn brain isolate, A β -amyloid deposits were identified as

418 early as two months pi, with the greatest number of deposits identified at three months pi.
419 As the number and size of amyloid deposits increased over time, the development of
420 AD-like pathology appeared to be progressive. This is an important issue as early initiating
421 events resulting in sporadic late-onset AD have not been addressed using genetically
422 modified transgenic models that principally emulate familial AD, not the more common
423 late-onset form of disease. Furthermore, animal models that mimic the sporadic late-onset
424 form of AD have been hampered by the lack of understanding of the primary factors that
425 promote the early deposition of A β -amyloid, however numerous experimentally induced
426 animal models utilizing direct injection of microbial products have been shown to induce
427 transient amyloid production and deposition (Krstic, *et al.* 2012; Erickson, *et al.* 2012).
428 Our current study with a respiratory isolate of Cpn supports the induction of transient
429 amyloid deposition and contrasts with our previous work suggesting that a brain isolate of
430 Cpn results in progressive amyloid accumulation.

431
432 Interestingly, a previous study did not identify substantial AD-like pathology in the brain
433 following infection with a respiratory isolate/laboratory strain of Cpn (TWAR 2043)
434 (Boelen, *et al.* 2007). Boelen and co-workers infected BALB/c mice, via intranasal
435 inoculation, and examined brain tissue at one and three months pi based upon the
436 assumption that TWAR 2043 and the human AD brain isolate 96-41 used by Little et al,
437 2004 would both induce a progressive pathology following infection. The number of
438 amyloid beta deposits was reported as 1 or 2 aggregates per section without a preference
439 for a certain brain region in the Boelen et al study, and the researchers indicated that Cpn
440 was not detected in the CNS at 1 or 3 months pi. In addition, both mock-infected and Cpn
441 infected mice displayed no difference in amyloid deposits. The clear difference noted from
442 the Little et al 2004 study of number and size of deposits was notably different from the
443 Boelen et al report. Boelen et al noted that these discrepancies could be due to the fact that
444 the TWAR 2043 Cpn strain used may have different virulence properties than the human
445 AD-brain isolate, 96-41. TWAR 2043 and 96-41 display different phenotypes with respect
446 to the ability to establish a persistent infection and the subsequent induction of pathology
447 within the brains of BALB/c mice.

448
449 Our current findings support the contention that isolates of Cpn may differ in their ability to
450 establish chronic or persistent infection and promote progressive pathology. Numerous
451 questions remain as to the nature of the organisms that typically infect the human
452 population. Pertinent issues, just to name a few, include: risk factors promoting infection at
453 specific sites in the body, spread into different tissues and organs following initial
454 infection, virulence factors expressed by the organism and/or host response, and age at
455 which infection occurs. With regards to age, a prior study of Cpn infection in older animals
456 suggests that older age at time of infection promotes the establishment of a brain infection
457 (Little, *et al.* 2005). Further, to address our current study that a modest inoculum of a
458 respiratory isolate of Cpn initiated specific but non-sustainable change in the brain
459 following intranasal inoculation, we preliminarily inoculated a small group of animals with
460 Cpn AR-39, either twice (days 0 and 30), or three times (days 0, 30 and 60) and sacrificed
461 at day 90, and found that individual BALB/c mice inoculated twice displayed 68 amyloid
462 deposits and those inoculated 3 times had 177 amyloid deposits (unpublished
463 observations). In comparison, mice receiving only a single intranasal inoculation as

464 observed in the current study at 3 months pi had an average of ~17 - 18 deposits (53
465 deposits/3 mice) (see table 1A). These preliminary observations would suggest that
466 multiple inocula of Cpn may exacerbate pathology in the brain, but further experiments are
467 required to clarify this. Furthermore, respiratory or blood-borne organisms may become
468 altered after invading different tissue sites including the brain and this may reflect biovar
469 and serovar differences with Cpn, although this remains to be determined. Future
470 sequencing analyses and specific characterization of different tissue and organ isolates
471 may help to resolve these issues.

472

473 In summary, host immune responses that limit or reduce Cpn replication and antigen
474 burden may effectively decrease Cpn as a primary stimulus for long-term production of
475 A β -amyloid in our experimental system. We propose that the difference in progressive
476 versus non-progressive AD-like pathology is due to as yet uncharacterized differences
477 between human AD-brain adapted isolates such as 96-41, and the respiratory isolates/
478 laboratory strains TWAR 2043 and AR-39. This implies that there are different virulence
479 factors including tissue tropism for different isolates of Cpn. Thus, the ability of the
480 organism to enter and persist in the central nervous system and potentiate a chronic
481 inflammatory response may be critical to its role in the initiation and maintenance of AD
482 pathogenesis.

483

484 **ACKNOWLEDGMENTS**

485 We would like to thank Ms. Gwendolyn Harley for cutting the paraffin-embedded tissues.
486 We also would like to thank the Bio-Medical Sciences department, the Center for Chronic
487 Disorders of Aging endowed through the Osteopathic Heritage Foundation, the PCOM
488 Division of Research, and the Adolph and Rose Levis Foundation for Alzheimer's disease
489 Research for their support of this project.

490

491 **AUTHOR AND CONTRIBUTORS**

492 **CSL** contributed to the conception and design of the work as well as the acquisition,
493 analysis and interpretation of the data and drafting the manuscript, **TAJ** contributed to the
494 acquisition, analysis and interpretation of the data, **CJH** contributed to design of the work
495 as well as the acquisition, analysis and interpretation of the data and editing the manuscript,
496 **HM** contributed to the acquisition and interpretation of the data, **DMA** contributed to the
497 conception of the work as well the interpretation of the data and editing the manuscript,
498 **BJB** contributed to the conception and design of the work as well as the analysis and
499 interpretation of the data and drafting the manuscript.

500

501 **REFERENCES**

- 502 Alkadhi, K. A., Srivareerat, M., and Tran, T. T. (2010). "Intensification of Long-Term
503 Memory Deficit by Chronic Stress and Prevention by Nicotine in a Rat Model of
504 Alzheimer's Disease." *Molecular and Cellular Neurosciences* 45 (3): 289-296.
505 doi:10.1016/j.mcn.2010.06.018.
- 506 Balin, B. J., Gerard, H. C., Arking, E. J., Appelt, D. M., Branigan, P. J., Abrams, J. T., et al.
507 (1998). "Identification and Localization of Chlamydia Pneumoniae in the Alzheimer's
508 Brain." *Medical Microbiology and Immunology* 187 (1): 23-42.

509 Boelen,E., Stassen,F. R., van der Ven,A. J., Lemmens,M. A., Steinbusch,H. P.,
510 Bruggeman,C. A., et al. (2007). "Detection of Amyloid Beta Aggregates in the Brain
511 of BALB/c Mice After Chlamydia Pneumoniae Infection." *Acta Neuropathologica*
512 114 (3): 255-261. doi:10.1007/s00401-007-0252-3.

513 Campbell,S., Yates,P. S., Waters,F., and Richmond,S. J. (1991). "Purification of
514 Chlamydia Trachomatis by a Simple and Rapid Filtration Method." *Journal of*
515 *General Microbiology* 137 (7): 1565-1569.

516 Erickson,M. A., Hartvigson,P. E., Morofuji,Y., Owen,J. B., Butterfield,D. A., and
517 Banks,W. A. (2012). "Lipopolysaccharide Impairs Amyloid Beta Efflux from Brain:
518 Altered Vascular Sequestration, Cerebrospinal Fluid Reabsorption, Peripheral
519 Clearance and Transporter Function at the Blood-Brain Barrier." *Journal of*
520 *Neuroinflammation* 9: 150-2094-9-150. doi:10.1186/1742-2094-9-150 [doi].

521 Fargo,K. and Bleiler,L. (2014). "Alzheimer's Association Report." *Alzheimer's &*
522 *Dementia : The Journal of the Alzheimer's Association* 10 (2): e47-92.

523 Gerard,H. C., Dreses-Werringloer,U., Wildt,K. S., Deka,S., Oszust,C., Balin,B. J., et al.
524 (2006). "Chlamydophila (Chlamydia) Pneumoniae in the Alzheimer's Brain." *FEMS*
525 *Immunology and Medical Microbiology* 48 (3): 355-366.
526 doi:10.1111/j.1574-695X.2006.00154.x.

527 Goate,A., Chartier-Harlin,M. C., Mullan,M., Brown,J., Crawford,F., Fidani,L., et al.
528 (1991). "Segregation of a Missense Mutation in the Amyloid Precursor Protein Gene
529 with Familial Alzheimer's Disease." *Nature* 349 (631191141581): 704-76.

530 Hall,A. M. and Roberson,E. D. (2012). "Mouse Models of Alzheimer's Disease." *Brain*
531 *Research Bulletin* 88 (1): 3-12. doi:10.1016/j.brainresbull.2011.11.017 [doi].

532 Hawkes,C. A., Deng,L., Fenili,D., Nitz,M., and McLaurin,J. (2012). "In Vivo Uptake of
533 Beta-Amyloid by Non-Plaque Associated Microglia." *Current Alzheimer Research* 9
534 (8): 890-901. doi:CAR-EPUB-20120123-021 [pii].

535 Hebert,L. E., Scherr,P. A., Bienias,J. L., Bennett,D. A., and Evans,D. A. (2003).
536 "Alzheimer Disease in the US Population: Prevalence Estimates using the 2000
537 Census." *Archives of Neurology* 60 (8): 1119-1122. doi:10.1001/archneur.60.8.1119
538 [doi].

539 Itzhaki,R. F., Wozniak,M. A., Appelt,D. M., and Balin,B. J. (2004). "Infiltration of the
540 Brain by Pathogens Causes Alzheimer's Disease." *Neurobiology of Aging* 25 (5):
541 619-627. doi:10.1016/j.neurobiolaging.2003.12.021.

542 Krstic,D., Madhusudan,A., Doehner,J., Vogel,P., Notter,T., Imhof,C., et al. (2012).
543 "Systemic Immune Challenges Trigger and Drive Alzheimer-Like Neuropathology in
544 Mice." *Journal of Neuroinflammation* 9: 151-2094-9-151.
545 doi:10.1186/1742-2094-9-151 [doi].

546 Kumar,A., Seghal,N., Naidu,P. S., Padi,S. S., and Goyal,R. (2007). "Colchicines-Induced
547 Neurotoxicity as an Animal Model of Sporadic Dementia of Alzheimer's Type."
548 *Pharmacological Reports : PR* 59 (3): 274-283.

549 Labak,M., Foniok,T., Kirk,D., Rushforth,D., Tomanek,B., Jasinski,A., et al. (2010).
550 "Metabolic Changes in Rat Brain Following Intracerebroventricular Injections of
551 Streptozotocin: A Model of Sporadic Alzheimer's Disease." *Acta*
552 *Neurochirurgica.Supplement* 106: 177-181. doi:10.1007/978-3-211-98811-4_32.

553 Levy-Lahad,E., Wijsman,E. M., Nemens,E., Anderson,L., Goddard,K. A., Weber,J. L., et
554 al. (1995). "A Familial Alzheimer's Disease Locus on Chromosome 1." *Science* 269
555 (522695365815): 970-93.

556 Little,C. S., Hammond,C. J., MacIntyre,A., Balin,B. J., and Appelt,D. M. (2004).
557 "Chlamydia Pneumoniae Induces Alzheimer-Like Amyloid Plaques in Brains of
558 BALB/c Mice." *Neurobiology of Aging* 25 (4): 419-429.
559 doi:10.1016/S0197-4580(03)00127-1 [doi]; S0197458003001271 [pii].

560 Little,C. S., Bowe,A., Lin,R., Litsky,J., Fogel,R. M., Balin,B. J., et al. (2005). "Age
561 Alterations in Extent and Severity of Experimental Intranasal Infection with
562 Chlamydomydia Pneumoniae in BALB/c Mice." *Infection and Immunity* 73 (3):
563 1723-1734. doi:73/3/1723 [pii]; 10.1128/IAI.73.3.1723-1734.2005 [doi].

564 McManus,R. M., Higgins,S. C., Mills,K. H., and Lynch,M. A. (2014). "Respiratory
565 Infection Promotes T Cell Infiltration and Amyloid-Beta Deposition in APP/PS1
566 Mice." *Neurobiology of Aging* 35 (1): 109-121.
567 doi:10.1016/j.neurobiolaging.2013.07.025 [doi].

568 Rogaev,E. I., Sherrington,R., Rogaeva,E. A., Levesque,G., Ikeda,M., Liang,Y., et al.
569 (1995). "Familial Alzheimer's Disease in Kindreds with Missense Mutations in a Gene
570 on Chromosome 1 Related to the Alzheimer's Disease Type 3 Gene." *Nature* 376
571 (654395379971): 775-78.

572 Wang,X. L., Zeng,J., Feng,J., Tian,Y. T., Liu,Y. J., Qiu,M., et al. (2014). "Helicobacter
573 Pylori Filtrate Impairs Spatial Learning and Memory in Rats and Increases
574 Beta-Amyloid by Enhancing Expression of Presenilin-2." *Frontiers in Aging
575 Neuroscience* 6: 66. doi:10.3389/fnagi.2014.00066 [doi].

576 Wisniewski,T. and Sigurdsson,E. M. (2010). "Murine Models of Alzheimer's Disease and
577 their use in Developing Immunotherapies." *Biochimica Et Biophysica Acta* 1802 (10):
578 847-859. doi:10.1016/j.bbadis.2010.05.004.

579 Wolfe,M. S. (2007). "When Loss is Gain: Reduced Presenilin Proteolytic Function Leads
580 to Increased Abeta42/Abeta40. Talking Point on the Role of Presenilin Mutations in
581 Alzheimer Disease." *EMBO Reports* 8 (2): 136-140. doi:7400896 [pii].

582
583 **Figure 1.** Recovery of viable *Chlamydia pneumoniae* from olfactory bulb and brain tissues
584 following intranasal infection. (A) At 1, 3 and 4 months post-infection, viable Cpn was
585 recovered from olfactory bulb tissue homogenates of 8 BALB/c mice, 3 of 3 mice at one
586 month pi, 3 of 3 mice at 3 months pi, and 2 of 3 mice at 4 months pi. (B) In contrast, only 1
587 mouse demonstrated viable Cpn from cerebral cortical tissue at any time; that being 1
588 mouse at 3 months pi. Viable Cpn was quantified as infectious forming units /ml of tissue
589 homogenate.

590 **Figure 2.** *Chlamydia pneumoniae* specific immunoreactivity in olfactory bulbs. Cpn
591 (AR-39) antigens were detected in olfactory bulb tissues at 1 month post-infection
592 following intranasal inoculation (arrows). A, B and C, D are representative images from 2
593 different mice infected with Cpn and labeled with a cocktail of anti-Cpn antibodies
594 (RDI-PROAC1p, M6600, 10C-27). E, F are representative images from mock infected
595 mice comparably immunolabeled. Mag bars A-F = 50µm.

596 **Figure 3.** *Chlamydia pneumoniae* specific immunoreactivity in the central nervous
597 system. Representative images of Cpn-specific antigen labeling in the brains of infected
598 mice at 1 month (panels A and B), 3 months (panels C and D), and 4 months (panels E and

599 **F)** post infection. The upper right corner of each image is a higher magnification image of
600 Cpn-specific antigen labeling as designated by the low magnification arrow. Mag bars =
601 50µm.

602 **Figure 4.** Beta amyloid Aβ 1-42 deposits in the CNS at 2 months pi following intranasal
603 infection with *Chlamydia pneumoniae* AR-39. Brains were examined by light microscopy
604 for the presence of Aβ 1-42 using a specific anti-Aβ 1-42 antibody. (**A-E**) Representative
605 images of Aβ 1-42-specific labeling (arrowheads) are shown within different regions of
606 this brain section. Ect (Entorhinal cortex), L Ent (Lateral entorhinal cortex), Th
607 (Thalamus), Prh (Perirhinal cortex), Cp (Cerebral peduncle). Mag bars (**A**) 100 µm (**B-E**)
608 20 µm.

609
610

Figure 1.TIF

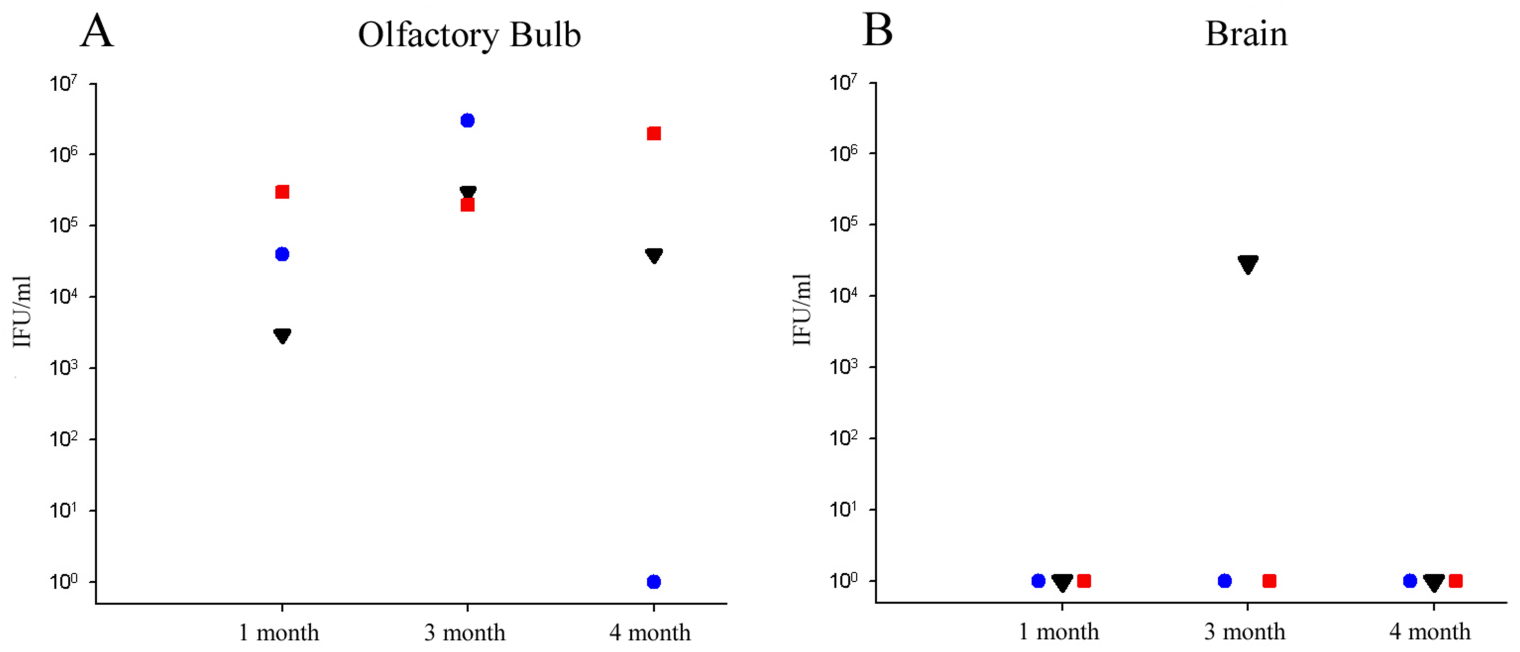


Figure 2.TIF

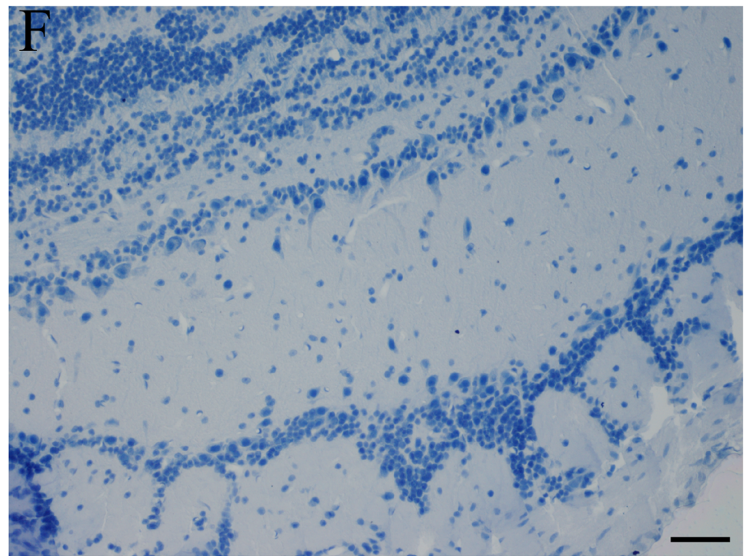
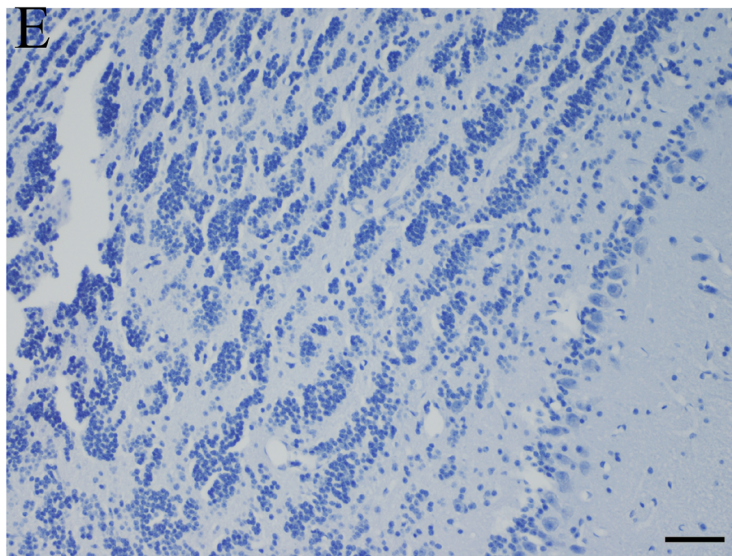
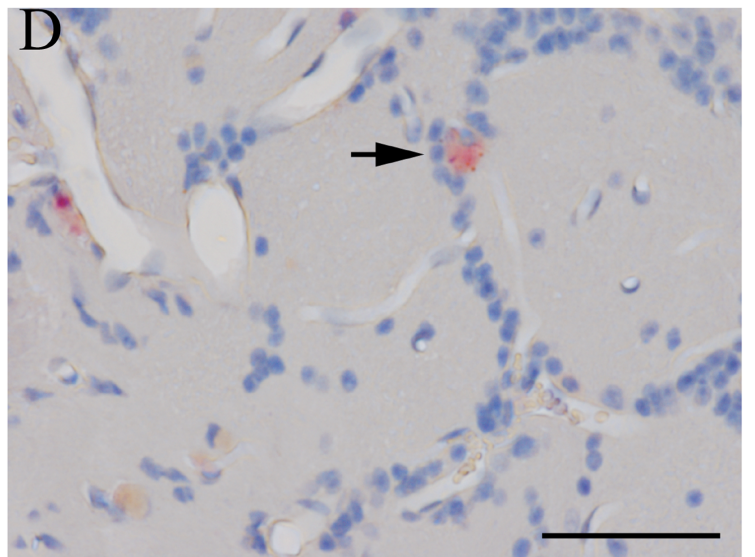
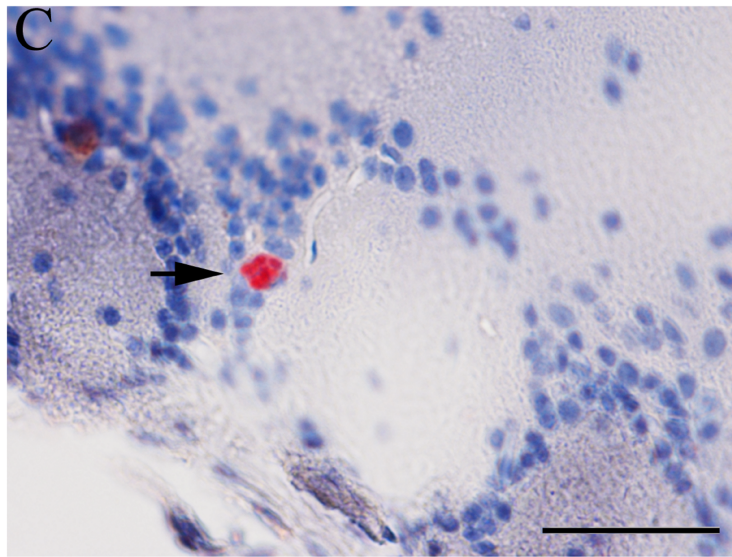
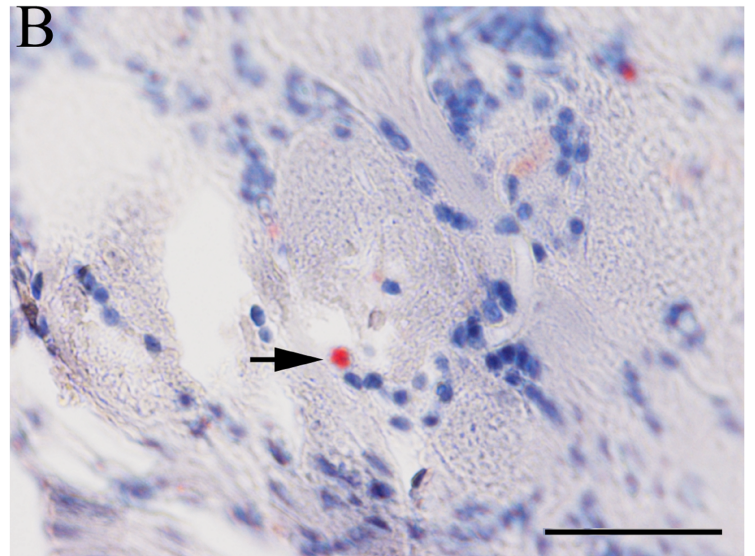
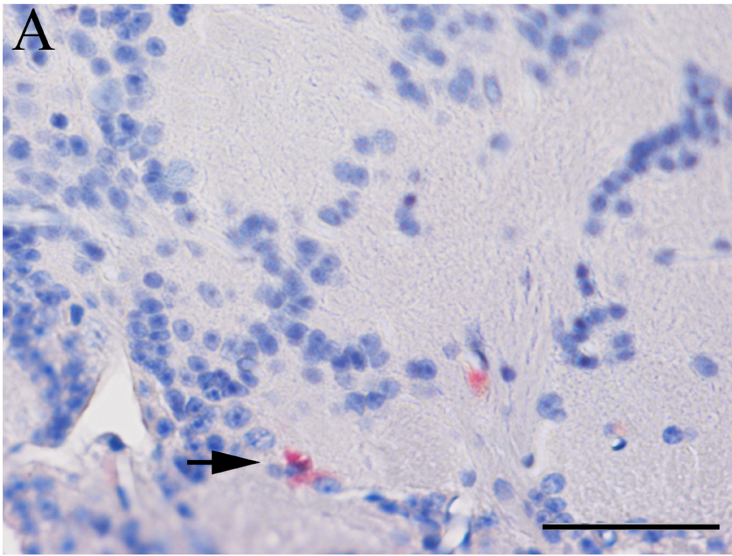


Figure 3.TIF

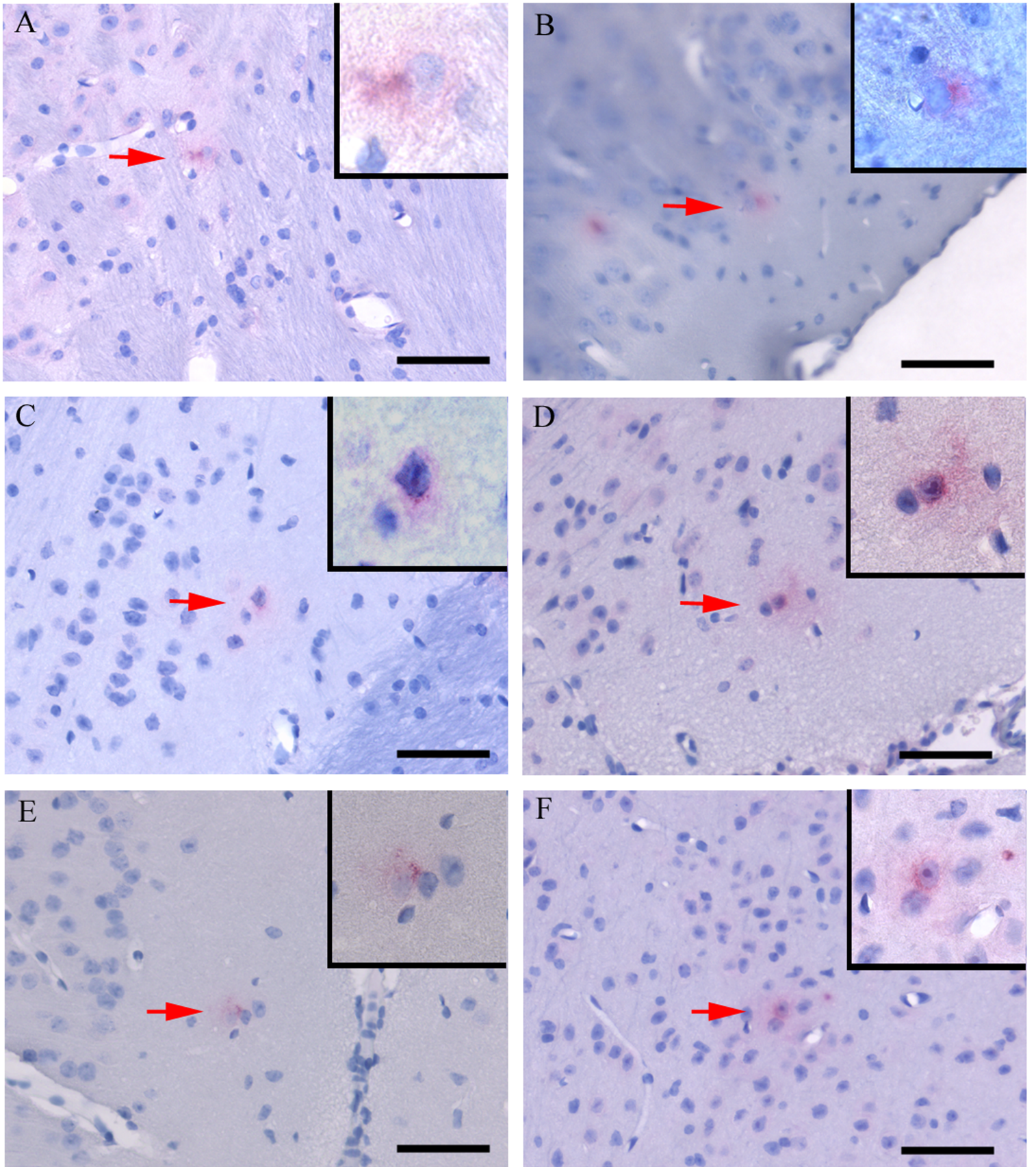


Figure 4.TIF

